HHS Public Access

Author manuscript

ChemMedChem. Author manuscript; available in PMC 2017 April 19.

Published in final edited form as:

ChemMedChem. 2016 April 19; 11(8): 893–899. doi:10.1002/cmdc.201500479.

Identification and Optimization of Anthranilic Acid-Based Inhibitors of Replication Protein A

Dr. James D. Patrone[a,d], **Nicholas F. Pelz**[a], **Brittney S. Bates**[a], **Prof. Elaine M. Souza-Fagundes**[a], **Bhavatarini Vangamudi**[a], **Demarco V. Camper**[a], **Dr. Alexey G. Kuznetsov**[a], **Carrie F. Browning**[a], **Dr. Michael D. Feldkamp**[a], **Dr. Andreas O. Frank**[a], **Benjamin A. Gilston**[a], **Prof. Edward T. Olejniczak**[a], **Prof. Olivia W. Rossanese**[a], **Prof. Alex G. Waterson**[b,c], **Prof. Walter J. Chazin**[a,c], and **Prof. Stephen W. Fesik**[a,b,c]

Stephen W. Fesik: stephen.fesik@vanderbilt.edu

[a]Department of Biochemistry, Vanderbilt University, Nashville, TN, USA, 37232

[b]Department of Pharmacology, Vanderbilt University, Nashville, TN, USA, 37232

[c]Department of Chemistry, Vanderbilt University, Nashville, TN, USA, 37232

Abstract

Replication Protein A (RPA) is an essential single-stranded DNA (ssDNA) binding protein that initiates the DNA damage response pathway through protein-protein interactions (PPIs) mediated by its 70N domain. The identification and use of chemical probes that can specifically disrupt these interactions is important for validating RPA as a cancer target. A high throughput screen (HTS) to identify new chemical entities was conducted and identified 90 hit compounds. From these initial hits, an anthranilic acid-based series was optimized using a structure-guided iterative medicinal chemistry approach to yield a cell penetrant compound that binds to RPA70N with an affinity of 812 nM. This compound (**20c**) is capable of inhibiting protein-protein interactions mediated by this domain.

Keywords

Replication Protein A; High throughput screening; Protein protein interactions; Medicinal chemistry; Hit optimization

Introduction

Replication Protein A (RPA), the primary single strand DNA (ssDNA) binding protein in eukaryotes, is essential for DNA replication, damage response and repair. In addition to binding to and protecting ssDNA from degradation, RPA recruits partner proteins involved in these processes. RPA is comprised of three subunits, each bearing OB-fold domains.[1,2] The N-terminal domain of the 70-kDa subunit (RPA70N) is one of two key sites that mediates the recruitment of partner proteins.[3] This domain is particularly important for the

Correspondence to: Stephen W. Fesik, stephen.fesik@vanderbilt.edu.

[d]Current address: Department of Chemistry, Rollins College, 1000 Holt Ave, Winter Park, FL, USA 32789

recruitment of DNA damage response proteins to sites of DNA damage via interaction with the RPA70N central basic cleft.[3–6]

Based on the key role of RPA70N-mediated protein-protein interactions (PPIs) in initiating the DNA damage response, it is possible that specific inhibition of this RPA function may represent an attractive pathway for therapeutic intervention in cancer. We and others are pursuing inhibitors of the RPA70N-mediated PPIs that do not interfere with the ability of RPA to bind to and protect ssDNA, as these would allow for further exploration of the role of RPA in checkpoint signaling, enable studies to confirm the therapeutic potential of RPA inhibition, and serve as a potential starting point for new cancer drugs.

Based on this unique opportunity for small molecule inhibitors of RPA as potential cancer therapeutics, research on RPA inhibitors has intensified over the last several years. Turchi and colleagues have identified dihydropyrazole 1 (Figure 1), which binds to a DNA-binding domain of RPA and disrupts its interaction with ssDNA.[7,8] Oakley and colleagues identified fumaropimaric acid (**2**; Figure 1), which was shown to disrupt both RPA70N-Rad9 and RPA70N-p53 interactions.[9,10] The Oakley laboratory has also reported on HAMNO (**3**, Figure 1), which was shown to inhibit RPA binding to RAD9 and cause increased replicative stress and cytotoxicity in cancer cells and slowed the progression of squamous cell carcinoma in a xenograft model.[11]

We have previously reported on the results of an NMR-based fragment screen to identify novel molecules that bind to RPA70N. This screen revealed several distinct chemotypes of fragments that bind to the domain. Remarkably, this single screen identified two distinct binding locations in the basic cleft of RPA70N (Site-1 and Site-2) which can be independently and simultaneously occupied by two different compounds.[12,13] From these results, we have also described the results of two optimization campaigns. Initially a fragment merging strategy was employed, resulting in triazole **4** (Figure 1), which bound to only one site in the basic cleft.[12] We have also described the results of a fragment linking strategy to generate compounds that span the entire cleft and incorporate features of two distinct fragment hits (**5**, Figure 1).[13] Here, we describe a different class of molecules that was identified using a high throughput screen (HTS) and further optimized using iterative medicinal chemistry and structure-based design.

Results and Discussion

Using a previously reported fluorescence polarization anisotropy (FPA) screening assay, 90,000 compounds from the Vanderbilt collection were screened at a single concentration of 30 μM for their ability to disrupt the binding of a fluorescently labeled ATRIP-derived probe to RPA70N.[14] This screen identified 674 compounds that displaced >10% of the probe from RPA70N at this concentration. These initial hits were further filtered to remove compounds that exhibited fluorescence interference and were prioritized for follow-up on the basis of the lack of potentially reactive chemical functionality and concordance with commonly accepted measures of drug-likeness.[15,16] After this analysis, concentration response curves were collected for 90 compounds to determine IC_{50} values from which K_d values were calculated.

Of these 90 compounds, 52 were identified with a K_d less than 100 μM. Several of the most potent hits are depicted in Figure 2.[3–6]

Compound **6**, with the highest ligand efficiency amongst the hit set, was briefly investigated. The results from this work were reported previously.[17] Because of the high lipophilicity of the series and generally flat SAR, further work on the series was halted. Notably, Turchi and coworkers previously described a series of inhibitors of the interaction of RPA and ssDNA with a chemical structure similar to compound **9**.[17] Compounds **7** and **8** were of relatively low interest. Compounds **10** and **11** are similar and together form an anthranilic acid-based series. SAR evident in the HTS hit set indicated the nitro group was essential for binding of ether-based exemplars such as **10**. Because of this, as well as the reasonably favorable combination of potency, ligand efficiency (LE), and the prospect of a modular synthetic route, we focused follow-up efforts onto sulfonamide variants such as compound **11**.

To guide the optimization of **11**, a co-crystal structure of compound **11** in complex with RPA70N was obtained (Figure 3). The binding mode of compound **11** shares several important contacts with the binding mode of the p53 peptide and our previously reported molecules. The 4-bromophenyl portion of the molecule occupies the hydrophobic Site-1 pocket (Figure 3A), but lies flat against the surface of RPA70N and sits in a much more shallow position as compared to compounds **4** and **5** (Figure 3C). The sulfonamide of the molecule appears to establish the proper geometry necessary to orient the 4-bromophenyl into Site-1. The middle phenyl ring occupies the center of the RPA70N cleft and overlays well with the indole moiety of the tryptophan of the p53 peptide[18] (Figure 3B) or the phenylalanine of a previously reported ATRIP-derived peptide[19]. The carboxylic acid of the anthranilic acid portion of the molecule engages in a charge-charge interaction with Arg41 of RPA70N, a common interaction amongst our fragments and linked small molecule inhibitors of RPA70N. In addition, compound **11** also makes a unique H bond interaction to Asn85 of RPA70N using the carbonyl oxygen of the amide bond. We hypothesized the amide in this molecule was important due to both this interaction with RPA and its ability to form an internal H bond with the anthranilic acid of the molecule, thus maintaining the planarity of the molecule in its binding pose.

Based upon the binding mode of hit molecule **11** and our previous knowledge of small molecules binding to RPA70N, we devised a strategy to improve potency by optimizing the hydrophobic interactions of each of the phenyl rings while maintaining the hydrophilic interactions of the amide and carboxylic acid of the molecule. The first goal was to optimize the phenyl sulfonamide portion of the molecule for binding to the hydrophobic pocket of Site-1. An initial compound library containing various phenyl substituents and phenyl replacements was constructed, using a combination of chemical synthesis and analog purchases. Despite the majority of the analogs being less potent than the original hit, this library provided important SAR insights (Table 1).

Analogs bearing a 3-Cl or 4-Cl (**18**, **19**) were equipotent with **11**, while non-halogen substituents such as 3-Me, 4-Me, or 4-OMe (**13, 14**, or **15**) were 5–8 fold less potent. In concordance with previously described SAR, analog **20** (3,4-diCl) displayed the best binding affinity of the initial set, showing a 4-fold improvement over **11**. Both of the chlorine atoms

were necessary, as replacing either or both with a methyl group (**21–23**) reduced binding affinity by 6–20 fold compared with **20**. Methylation of the sulfonamide was not tolerated, as all methylated analogs were 2–5 fold less potent than the des-methyl analogs (data not shown). Replacement of the phenyl ring with saturated ring systems (**27–32**, **34**, and **35**) in attempts to increase the hydrophobic interactions and increase the sp^3 character of the molecule, were unsuccessful, as all analogs were 2–10 fold lower in binding affinity to RPA70N. Surprisingly, the 3,4-diCl substituted biphenyl **25** had an affinity of 4 μM, despite its increased size within Site-1. However, derivatives of this molecule were not pursued further due to poor LE (0.20) and cLogP (6.08), as well as potential solubility limitations.

To explore the SAR around the phenyl ring of the anthranilic acid portion of the molecule, a library of analogs was synthesized with varying R^2 substituents, while R^1 was fixed as either 3,4-diCl, 3-Cl, or 4-Br. From this library, several clear SAR tends emerged (Table 2). Halogen R^2 options were more beneficial at the 4-position, as compared to the 5-position, leading to an improvement of 2–10 fold. This observation can be rationalized from the co-crystal structure, in which one can envision the 5-position substitution clashing with the lip of the cleft, whereas the 4-position substitution is oriented towards a hydrophobic gap. A 5-Cl substitution at R^2 consistently led to poor physicochemical properties, such as limiting solubility, as evidenced by precipitation under the assay conditions.

The most effective option at R^2 for all three different R^1 substitutions was replacement of the anthranilic acid phenyl ring with a naphthyl moiety (**11l**, **18l**, **20l**). These analogs displayed binding affinities of 1–4 μM. Based on the co-crystal structure of **11**, the naphthyl substitution most likely occupies the hydrophobic space adjacent to both the 4- and 5-positions. The analog with the best binding affinity (**20c**), however, contained a 3,4-diCl R^1 substitution and a 4-Br R^2 substitution. This analog was slightly superior to the R2 = naphthyl analog (**20l**) and had a more attractive LE (0.27 compared to 0.24 for **20l**). Further, compound **20c** represents the best binding affinity yet observed for a molecule with only one acidic moiety.

The final strategy to optimize compound **11** was exploration of several substituents at R^3 on the middle phenyl ring. However, several planned analogs (R^3 = Cl, Br, or OMe, for example) were synthetically intractable, since intermediates required for the synthesis of these molecules were unstable under the conditions necessary for sulfonamide formation or saponification. Despite these challenges, several alkyl analogs were obtained (Table 3). The des-methyl analog **20m** was 2-fold less potent than compound **20**. Further extension of the methyl to an ethyl (**20n**) or isopropyl group (**20o**) showed marginal improvements in affinity (K_d = 4 and 5 μM, respectively). However, this slight gain in potency was offset by a decrease in solubility of these analogs, with both **20n** and **20o** showing some evidence of precipitation at the highest concentrations under the assay conditions.

Using a standard fluorescence-based DNA binding assay, we established that compound **20c** does not affect ssDNA binding to RPA; the K_d value for ssDNA binding to RPA70AB in the RPA70NAB construct was the same in the absence and presence of the compound. Thus, **20c** appears to bind selectively to the RPA70N domain. Further, compound **20c** was taken forward for characterization in cellular studies. The molecule was found to possess very high

protein binding (99.8%), but also exhibits high permeability (P^{app} A–B value of 29.2×10^{-6} cm/sec in the Caco-2 line) relative to our previously reported compounds. Studies to define the cellular activity of this compound are underway and will be reported in due course.

Chemistry

The synthesis of the anthranilic acid-based inhibitors **11–36** utilized a modular route, allowing for the introduction of diversity at each step and only one chromatographic purification.[21] The synthesis begins with an aromatic sulfonylation, upon treating a *para*-substituted benzoic with chlorosulfonic acid. The carboxylic acid (**40–42**) is converted to an acid chloride and the methyl ester of the appropriate anthranilic acid is added to afford sulfonyl chlorides in greater than 90% yield. After a water work up, the final substituted phenyl ring is added to the sulfonyl chloride by the addition of the appropriate substituted aniline. This is followed by saponification of the methyl ester to yield the desired analog.

Conclusions

We have conducted a high throughput screen and initial compound optimization towards the discovery of new and selective chemical probes to validate inhibition of the protein-protein interactions mediated by RPA70N. Inhibitor **11** was initially identified as an attractive starting point for structure-based optimization. Subsequent optimization using an iterative medicinal chemistry process and structure-based design principles led to the discovery of **20c**, which binds to RPA70N with an affinity of 812 nM and displays adequate permeability and solubility characteristics for use in cellular studies.

Experimental Section

Chemistry

General Methods—All chemicals, reagents, and solvents were used as purchased from commercial sources, without further purification. All NMR spectra were recorded at room temperature on a 400 MHz Bruker spectrometer with a DRX-400 console, a 500 MHz Bruker spectrometer with a DRX-500 console, or a 600 MHz Bruker spectrometer with an AV-II console. ^{1}H chemical shifts are reported in δ values in ppm downfield with the deuterated solvent as the internal standard. Data are reported as follows: chemical shift, multiplicity (s = singlet, d = doublet, t = triplet, q = quartet, br = broad, m = multiplet, ovlp = overlap), coupling constant (Hz), and integration. Low-resolution mass spectra were obtained on an Agilent 1200 series 6140 mass spectrometer with electrospray ionization. All samples were of ≥90% purity as analyzed by LC−UV/vis−MS. Analytical HPLC was performed on an Agilent 1200 series with UV detection at 214 and 254 nm along with ELSD detection. LC−MS parameters were as follows: Phenomenex-C18 Kinetex column, 50 mm × 2.1 mm, 2 min gradient, 5% to 100% (H_2O/MeCN with 0.1% TFA). Preparative purification was performed on a Gilson HPLC (Phenomenex-C18, 100 mm × 30 mm, 10 min gradient, (H_2O/MeCN with 0.1% TFA) or by automated flash column chromatography (Teledyne Isco, Inc. Combiflash Rf).

General Procedure for anthranilic acid-based inhibitors

The anthanilic-based inhibitors **11a–l, 12–17, 18a–l, 19, 20a–p, and 21–36** were prepared by the similar procedures. This procedure is exemplified for compound **11**.[18]

3-(Chlorosulfonyl)-4-methylbenzoic acid 40—4-methylbenzoic acid 37 (1.0 g, 7.35 mmol, 1 eq) was dissolved in chlorosulfonic acid (10 mL). The reaction was heated t reflux and stirred overnight. The next day, the reaction was cooled to room temperature and then poured onto ice. The solid was filtered, dissolved in DCM, and washed with 1M HCl. The DCM layer was then driesd (Na2SO4) and evaporated in vacuo to give the desired product 37 (1.22 g, 71%). ^{1}H-NMR (600 MHz, DMSO-d_6): δ = 8.32 (d, *J* = 1.9 Hz, 1 H), 7.77 (dd, *J* = 2.0 Hz, 7.7 Hz, 1 H), 7.26 (d, *J* = 7.9 Hz, 1 H), 2.58 (s, 3H). ^{13}C-NMR (125 MHz, DMSO-d_6): δ =167.2, 146.4, 141.2, 131.2, 129.6, 127.7, 127.5, 20.3. MS (ESI) $[M + H]^+$ *m/z* = 234.9.

Methyl 2-(3-(chlorosulfonyl)-4-methylbenzamido)benzoate 43a—The intermediate **40** (235 mg, 1 mmol, 1 eq) was dissolved in thionyl chloride (4 mL). The reaction was heated to 75°C and stirred for 4 hours. Solvents were removed *in vacuo*. The resulting syrup was dissolved in toluene (3 × 5 mL) and evaporated. The product was taken forward without further purification.

The appropriate methyl-2-aminobenzoate (151 mg, 1 mmol, 1 eq) was dissolved in THF (4 mL) and NaH (40 mg, 1 mmol, 1 eq) was added and stirred for 20 min. The acyl chloride (1 mmol, 1 eq) was added and the reaction was stirred at rt for 2 hours. The reaction was diluted with DCM and washed with water. The DCM layer was dried (Na_2SO_4) and then evaporated *in vacuo*. The residue was taken forward without further purification (367 mg, quantitative). ^{1}H-NMR (600 MHz, DMSO-d_6): δ = 8.57 (dd, *J* = 0.8 Hz, 8.5 Hz, 1 H), 8.39 (d, *J* = 2.1 Hz, 1 H), 8.00 (dt, *J* = 1.9 Hz, 8.0 Hz, 1 H), 7.80 (dd, *J* = 2.1 Hz, 7.8 Hz, 1 H), 7.67 (m, 1 H), 7.37 (d, *J* = 7.9 Hz, 1 H), 7.22 (m, 1 H), 3.90 (s, 3 H), 2.62 (s, 3 H). ^{13}C-NMR (150 MHz, DMSO-d_6): δ = 168.0, 164.7, 146.9, 140.5, 140.3, 134.3, 131.4, 131.1, 130.8, 127.0, 125.7, 123.3, 120.9, 117.1, 52.7, 20.2. MS (ESI) $[M + H]^+$ *m/z* = 368.0.

2-(3-(*N*-(4-bromophenyl)sulfamoyl)-4-methylbenzamido)benzoic acid 11—The sulfonyl chloride **43a** (62 mg, 0.17 mmol, 1 eq) was dissolved in toluene (2 mL). The 4-bromoaniline (86 mg, 0.5 mmol, 3 eq) is added and the rxn is stirred at 70°C overnight. The solvents were removed *in vacuo*. The resulting residue was dissolved in DCM and washed with water. The DCM layer was evaporated *in vacuo* and the residue was dissolved in THF (2 mL) and 2M LiOH (0.5 mL) was added. The reaction was stirred at 55°C for 2 hours. The reaction was neutralized with 2 M HCl (0.5 mL) and the solvents were removed *in vacuo*. The residue was purified via preparative HPLC to give the desired product (23 mg, 28%). ^{1}H-NMR (600 MHz, DMSO-d_6): δ = 10.78 (s, 1 H), 8.67 (dd, *J* = 0.8 Hz, 8.4 Hz 1 H), 8.52 (d, *J* = 1.9 Hz, 1 H), 8.08-8.05 (m, 2 H), 7.68 (m, 1 H), 7.62 (d, *J* = 8.1 Hz, 1 H), 7.43-7.41 (m, 2 H), 7.24 (m, 1 H), 7.09-7.06 (m, 2 H), 3.39 (broad s, 1 H), 2.66 (s, 3 H). ^{13}C-NMR (150 MHz, DMSO-d_6): δ = 170.6, 163.5, 141.6, 141.3, 138.3, 137.1, 134.9, 134.1, 133.0, 132.7, 131.9, 131.8, 128.7, 123.8, 121.5, 120.5, 117.2, 116.2, 20.2. MS (ESI) $[M + H]^+$ *m/z* = 489.1.

2-(3-(*N*-(3-chlorophenyl)sulfamoyl)-4-methylbenzamido)benzoic acid 18— Synthesized according to procedure for **11** in 42% yield. ^{1}H-NMR (600 MHz, DMSO-d_6): δ = 10.88 (s, 1 H), 8.67 (dd, *J* = 0.9 Hz, 8.4 Hz 1 H), 8.55 (d, *J* = 1.9 Hz, 1 H), 8.09-8.06 (m, 2 H), 7.68 (m, 1 H), 7.63 (d, *J* = 8.1 Hz, 1 H), 7.27-7.23 (m, 2 H), 7.12-7.09 (m, 2H), 7.04 (m, 1H), 3.40 (broad s, 1 H), 2.67 (s, 3 H). ^{13}C-NMR (150 MHz, DMSO-d_6): δ = 170.1, 162.9, 141.2, 140.7, 138.8, 137.8, 134.4, 133.6, 133.5, 132.5, 132.4, 131.4, 131.3, 131.1, 128.2, 123.4, 123.3, 120.0, 118.1, 116.9, 19.7. MS (ESI) $[M + H]^+$ *m/z* = 445.2.

4-Bromo-2-(3-(*N*-(3-chlorophenyl)sulfamoyl)-4-methyl benzamido)benzoic acid 18c—Synthesized according to procedure for **11** in 34% yield. ^{1}H-NMR (600 MHz, DMSO-d_6): δ = 10.91 (s, 1 H), 8.93 (d, *J* = 2.0 Hz 1 H), 8.55 (d, *J* = 2.0 Hz, 1 H), 8.06 (dd, *J* = 1.8 Hz, 7.4 Hz, 1 H), 7.99 (d, *J* = 8.4 Hz 1 H), 7.63 (d, *J* = 8.0 Hz, 1 H), 7.44 (dd, *J* = 2.0 Hz, 8.6 Hz, 1 H), 7.27 (t, *J* = 8.1 Hz 1 H), 7.13-7.10 (m, 2 H), 7.05 (m, 1 H), 3.42 (broad s, 1 H), 2.68 (s, 3 H). ^{13}C-NMR (150 MHz, DMSO-d_6): δ = 168.0, 161.5, 140.1, 139.8, 137.1, 136.2, 132.1, 131.9, 131.3, 130.3, 129.8, 129.5, 126.6, 126.1, 124.5, 121.8, 120.6, 116.5, 115.2, 114.2, 18.1. MS (ESI) $[M + H]^+$ *m/z* = 568.9.

4-Bromo-2-(3-(*N*-(3,4-dichlorophenyl)sulfamoyl)-4-methyl benzamido)benzoic acid 20c—Synthesized according to procedure for **11** in 42% yield. ^{1}H-NMR (600 MHz, DMSO-d_6): δ = 11.05 (s, 1 H), 8.92 (d, *J* = 2.1 Hz 1 H), 8.53 (d, *J* = 1.9 Hz, 1 H), 8.06 (dd, *J* = 1.9 Hz, 7.9 Hz, 1 H), 7.98 (d, *J* = 8.5 Hz 1 H), 7.64 (d, *J* = 8.2 Hz, 1 H), 7.50 (d, *J* = 8.8 Hz 1 H), 7.43 (dd, *J* = 2.1 Hz, 8.5 Hz, 1 H), 7.28 (d, *J* = 2.6 Hz 1 H), 7.12 (dd, *J* = 2.6 Hz, 8.9 Hz, 1 H), 3.39 (broad s, 1 H), 2.67 (s, 3 H). ^{13}C-NMR (150 MHz, DMSO-d_6): δ = 169.6, 163.1, 141.8, 141.5, 137.6, 137.4, 133.8, 133.0, 132.1, 131.6, 131.6, 131.4, 128.2, 127.7, 126.1, 125.6, 122.2, 119.8, 118.3, 115.8, 19.7. MS (ESI) $[M + H]^+$ *m/z* = 556.9.

Fluorescence Polarization Anisotropy (FPA) Assays

90,000 compounds from the Vanderbilt Institute of Chemical Biology compound collection were screened at the High Throughput Screening core at a single concentration of 30 mM for their ability to disrupt the binding of an ATRIP-based probe to RPA70N. The protocol is described in full detail in Souza-Fagundes, E.M., et al., *Anal Biochem*, 2012.[14]

FPA competition assays were conducted as previously described with minor modifications.[12,14] Compounds were diluted in a 10-point, 3-fold serial dilution scheme in DMSO for a final concentration range of 500 – 0.025 μM. Compounds were added to assay buffer (50 mM HEPES, 75 mM NaCl, 5 mM DTT, pH 7.5) containing FITC-labeled probe and appropriate RPA70 protein in a final reaction volume of 50 μL containing 5% DMSO. All assays were conducted using a protein concentration equal to 1× K_d for the protein/probe interaction. Therefore, competition for binding to RPA70N was measured using either the FITC-ATRIP peptide (FITC-Ahx-DFTADDLEELDTLAS-NH_2; 50 nM with 6 μM RPA70N) or the FITC-ATRIP2 peptide (FITC-Ahx-DFTADDLEEWFAL-NH_2; 25 nM with 350 nM RPA70N). Binding to RPA70NAB was measured using 200 nM RPA70NAB and 25 nM FITC-ATRIP2. Following incubation for 1h, emission anisotropy was measured using the EnVision plate reader (Perkin Elmer). IC_{50} values were generated using a four-parameter

dose-response (variable slope) equation in XLfit and were converted to K_d values. Reported K_d values are the average of two independent experiments, run in duplicate.

X-ray crystal structures of complexes with RPA70N—Crystals of the E7R mutant of RPA70N were grown as described previously.[20] X-ray diffraction data were collected at sector 21 (Life Sciences Collaborative Access Team, LS-CAT) of the Advanced Photon Source (Argonne, IL). All data were processed by HKL-2000.[22] E7R crystallized in space group $P2_12_12_1$ and contained one molecule in the asymmetric unit. Initial phases were obtained by molecular replacement with PHASER[23] using the structure of the free protein (4IPC) as a search model. Iterative cycles of model building and refinement were performed using COOT[24] and PHENIX.[25] The structure of compound **20c** bound to E7R are deposited at the Protein Data Bank under accession code 5E7N. The program Pymol (Schrödinger) was used to visualize and analyze the structures.

Protein Binding and Cellular Permeability Studies—The studies on **20c** were performed by Absorption Systems, a preclinical contract research organization. Brief details of the studies can be could in the Supplementary Information.

Supplementary Material

Refer to Web version on PubMed Central for supplementary material.

Acknowledgments

We would like to thank Dr. David Cortez for his intellectual contributions in the conception of this project. We would also like to acknowledge the Vanderbilt High Throughput Screening Core, an institutionally supported facility in which some of these experiments were performed and whose staff provided invaluable assistance.

Funding of this research was provided in part by NIH grants 5DP1OD006933/8DP1CA174419 (NIH Director's Pioneer Award) to S.W.F., R01GM065484 and P01 CA092584 to W.J.C., and ARRA stimulus grant (5RC2CA148375) to Lawrence J. Marnett and funding from the National Council for Scientific and Technological Development – CNPq and Federal University of Minas Gerais/Brazil to E.M.S.-F.. A.O.F. was supported by a Deutscher Akademischer Austausch Dienst (DAAD) postdoctoral fellowship, J.D.P. by the NIH NRSA postdoctoral fellowship (F32 CA174315-02) and M.D.F. by the NIH NRSA postdoctoral fellowship (F32 ES021690-01).

References

1. Wold MS. Annu. Rev. Biochem. 1997; 66:61. [PubMed: 9242902]
2. Wold MS, Kelly T. P. Natl. Acad. Sci. USA. 1988; 85:2523.
3. Xu X, Vaithiyalingam S, Glick GG, Mordes DA, Chazin WJ, Cortez D. Mol. Cell Biol. 2008; 28:7345. [PubMed: 18936170]
4. Fanning E, Klimovich V, Nager AR. Nucleic Acids Res. 2006; 34:4126. [PubMed: 16935876]
5. Cortez D, Guntuku S, Qin J, Elledge SJ. Science. 2001; 294:1713. [PubMed: 11721054]
6. Cimprich KA, Cortez D. Nat. Rev. Mol. Cell Biol. 2008; 9:616. [PubMed: 18594563]
7. Andrews BJ, Turchi JJ. Mol. Cancer Ther. 2004; 3:385. [PubMed: 15078981]
8. Shuck SC, Turchi JJ. Cancer Res. 2010; 70:3189. [PubMed: 20395205]
9. Glanzer JG, Liu SQ, Oakley GG. Bioorgan. Med. Chem. 2011; 19:2589.
10. Glanzer JG, Carnes KA, Soto P, Liu S, Parkhurst LJ, Oakley GG. Nucleic Acids Res. 2013; 41:2047. [PubMed: 23267009]
11. Glanzer JG, Liu S, Wang L, Mosel A, Peng A, Oakley GG. Cancer Res. 2014; 74:5165. [PubMed: 25070753]

12. Patrone JD, Kennedy JP, Frank AO, Feldkamp MD, Vangamudi B, Pelz NF, Rossanese OW, Waterson AG, Chazin WJ, Fesik SW. ACS Med. Chem. Lett. 2013; 4:601. [PubMed: 23914285]
13. Frank AO, Feldkamp MD, Kennedy JP, Waterson AG, Pelz NF, Patrone JD, Vangamudi B, Camper DV, Rossanese OW, Chazin WJ, Fesik SW. J. Med. Chem. 2013; 56:9242. [PubMed: 24147804]
14. Souza-Fagundes EM, Frank AO, Feldkamp MD, Dorset DC, Chazin WJ, Rossanese OW, Olejniczak ET, Fesik SW. Anal. Biochem. 2012; 421:742. [PubMed: 22197419]
15. Baell JB, Holloway GA. J. Med. Chem. 2010; 53:2719. [PubMed: 20131845]
16. Lipinski CA, Lombardo F, Dominy BW, Feeney PJ. Adv. Drug Deliver. Rev. 1997; 23:3.
17. Granadillo VJ, Earley JN, Shuck SC, Georgiasdis MM, Fitch RW, Turchi JJ. J. Nucleic Acids. 2010:1.
18. Bochkareva E, Kasutov L, Ayed A, Yi G-S, Pineda-Lucena A, Liao JCC, Okorokov AL, Milner J, Arrowsmith CH, Bochkarev A. P. Natl. Acad. Sci. USA. 2005; 102:15412.
19. Frank AO, Vangamudi B, Feldkamp MD, Souza-Fagundes EM, Luzwick JW, Cortez D, Olejniczak ET, Waterson AG, Rossanese OW, Chazin WJ, Fesik SW. J. Med. Chem. 2014; 57:2455. [PubMed: 24491171]
20. Feldkamp MD, Frank AO, Kennedy JP, Patrone JD, Vangamudi B, Waterson AG, Fesik SW, Chazin WJ. Biochemistry. 2013; 52:6515. [PubMed: 23962067]
21. Thorarensen, A.; Ruble, CJ.; Romero, DL. (Pfizer Inc.), Pub No. WO2004018428 A3. 2004.
22. Otwinowski ZM, W. Methods Enzymol. 1997; 276:307.
23. Winn MD, Ballard CC, Cowtan KD, Dodson EJ, Emsley P, Evans PR, Keegan RM, Krissinel EB, Leslie AG, McCoy A, McNicholas SJ, Murshudov GN, Pannu NS, Potterton EA, Powell HR, Read RJ, Vagin A, Wilson KS, S K. Acta Crystallogr. 2011; D67:235.
24. Emsley P, Cowtan K. Acta Crystallogr. 2004; D60:2126.
25. Adams PD, Afonine PV, Bunkoczi G, Chen VB, Davis IW, Echols N, Headd JJ, Hung LW, Kapral GJ, Grosse-Kunstleve RW, McCoy AJ, Moriarty NW, Oeffner R, Read RJ, Richardson DC, Richardson JS, Terwilliger TC, Zwart PH. Acta Crystallogr. 2010; D66:213.

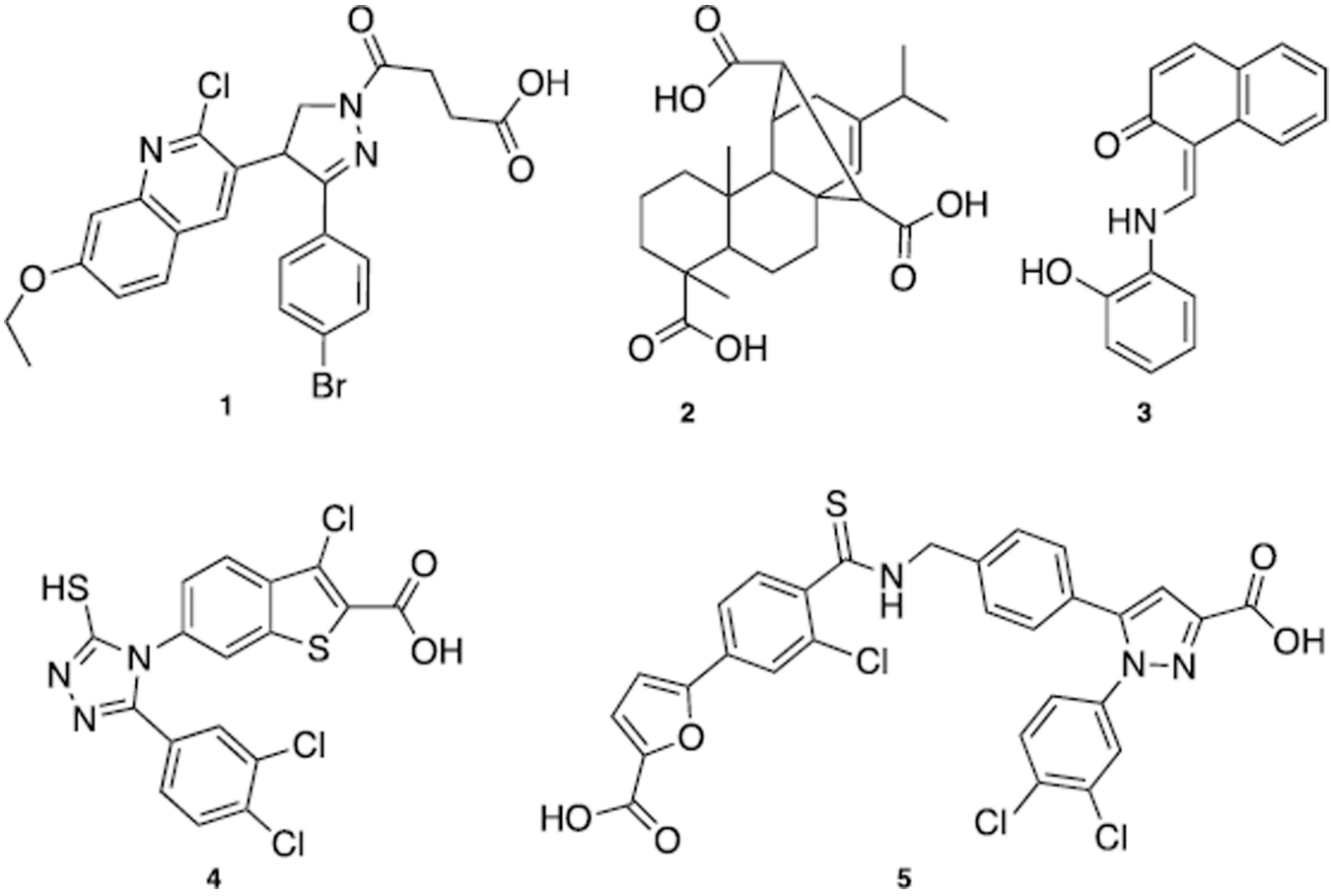

Figure 1.
Previously reported RPA PPI inhibitors.

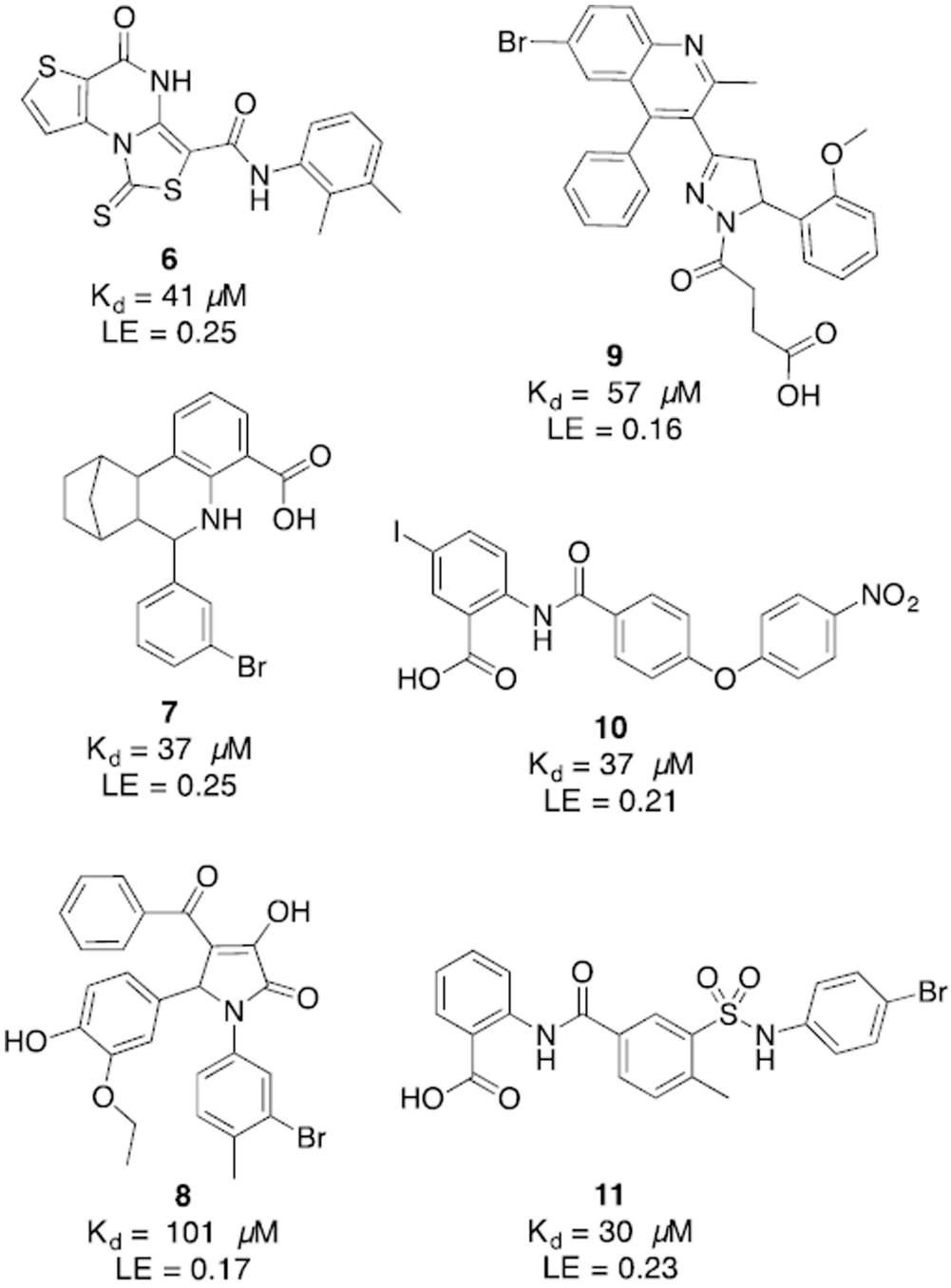

Figure 2.
Selected HTS hit compounds.

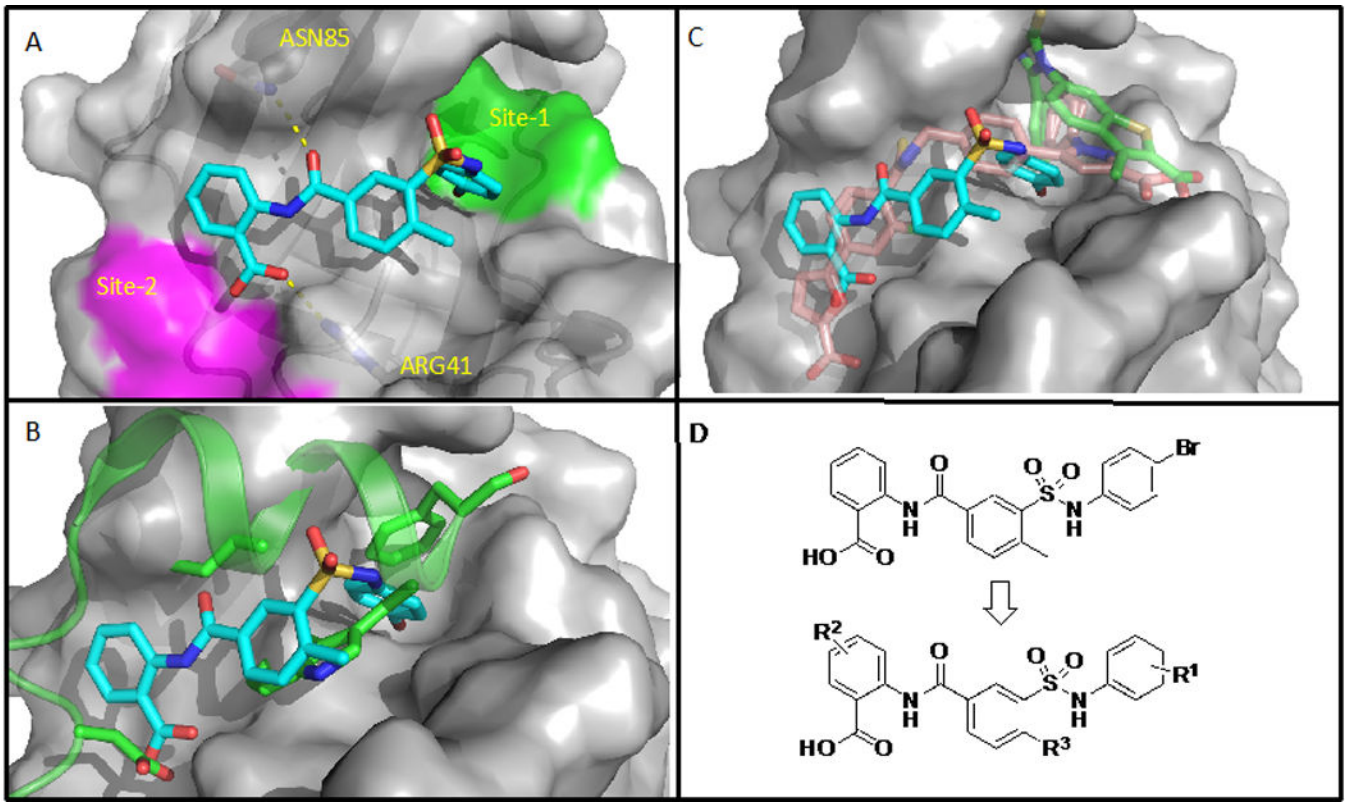

Figure 3.

A) Compound **11** in complex with RPA70N. B) Compound **11** in complex with RPA70N with p53 peptide[18] superimposed. C) Compound **11** in complex with RPA70N with compounds **4** and **5** superimposed. D) SAR strategy for compound **11**.

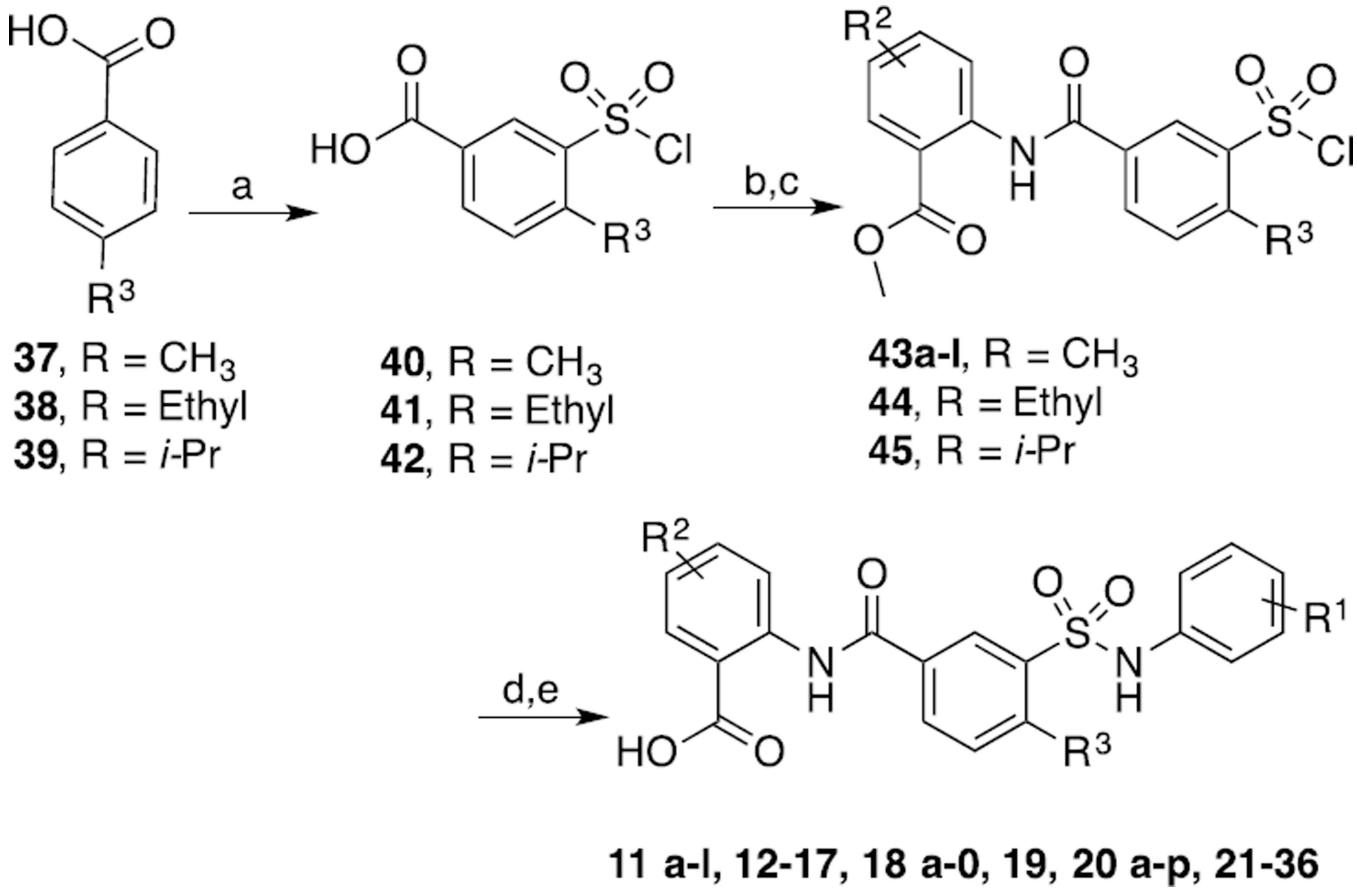

Scheme 1.

General synthesis of anthranilic acid-based RPA inhibitors. Reagents and conditions: a) Chlorosulfonic acid, reflux, 16 hrs; b) thionyl chloride, 75°C, 4 hrs; c) methyl 2-aminobenzoate-R_2, THF, 12 hrs d) aniline-R_1, toluene, 70°C, 12hrs; e) 2M LiOH, 55°C, 2 hrs.

Table 1

Structure activity relationships in Site-1.

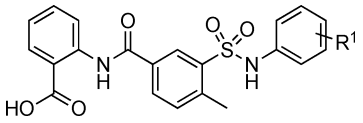

Compd	R_1	K_d (μM)[a]	LE[c]
11	4-Br	30±6	0.21
12	H	156 ± 11	0.18
13	3-Me	165 ± 34	0.18
14	4-Me	196	0.17
15	4-OMe	234 ± 3	0.16
16	4-ethyl	95 ± 6.5	0.18
17	4-isopropyl	76 ± 5.5	0.17
18	3-Cl	29 ± 2	0.21
19	4-Cl	44 ± 0	0.20
20	3,4-diCl	7 ± 3	0.23
21	3,4-diMe	150 ± 11	0.17
22	3-Cl, 4-Me	43 ± 3.5	0.19
23	3-Me, 4-Cl	58 ± 11	0.18
24	2-naphthyl[b]	83 ± 8	0.17
25	3',4'-dichloro-[1,1'-biphenyl]-3-amine[b]	4 ± 0.5	0.20
26	indane[b]	106 ± 5.5	0.17
27	cyclopentyl[b]	>250	0.18
28	cyclohexyl[b]	193	0.18
29	4-aminotetrahydropyran[b]	>250	n.c. [d]
30	cycloheptyl[b]	110 ± 4	0.19
31	trans-4-Me cyclohexyl[b]	81 ± 10	0.20
32	cyclohexylmethyl[b]	126 ± 1	0.19
33	benzyl[b]	>250	n.c.[d]
34	azepane[b]	208	0.18
35	octahydrocyclopenta[*c*]pyrrole[b]	222 ± 28	0.17
36	isoindoline[b]	>250	n.c. [d]

[a] Average K_d values (n=2) calculated using Cheng-Prusoff equation from IC_{50} values measured in FPA competition assay.

[b] Entire ring system replaces the phenyl.

[c] LE values calculated using LE = 1.4*pK_d/HAC, using the FPA data.

[d] n.c. = not calculated.

Table 2

SAR of anthranilic acid ring substituents.

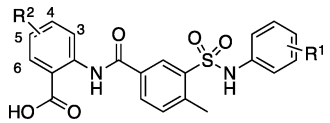

Compd	R_1	R_2	K_d (μM)[a]	LE[c]	Compd	R_1	R_2	K_d (μM)[a]	LE[c]
20	3,4-diCl	H	7 ± 3	0.23	**18g**	3-Cl	5-Me	30 ± 1	0.20
11a	4-Br	4-Cl	25 ± 2	0.21	**18h**	3-Cl	6-Me	134 ± 1	0.17
11b	4-Br	5-Cl	ppt[d]	n.c. [e]	**18i**	3-Cl	4,5-diMe	>250	n.c. [e]
11c	4-Br	4-Br	18 ± 1.5	0.22	**18j**	3-Cl	5-Ethyl	6 ± .37	0.23
11d	4-Br	5-Br	20 ± 3.5	0.21	**18k**	3-Cl	5-*i*Pr	7 ± .25	0.22
11e	4-Br	4-F	34 ± 3.5	0.20	**18l**	3-Cl	4,5 Naphthyl[b]	4 ± 0.1	0.22
11f	4-Br	5-F	48 ± 8	0.20	**20a**	3,4-diCl	4-Cl	4 ± 1	0.24
11g	4-Br	5-Me	33 ± 2	0.20	**20b**	3,4-diCl	5-Cl	ppt[d]	n.c. [e]
11h	4-Br	6-Me	73 ± 0.5	0.19	**20c**	3,4-diCl	4-Br	0.81 ± 0.3	0.27
11i	4-Br	4,5-diMe	>250	n.c. [e]	**20d**	3,4-diCl	5-Br	8 ± 1.3	0.22
11j	4-Br	5-Ethyl	9 ± 0.83	0.22	**20e**	3,4-diCl	4-F	8 ± 2	0.22
11k	4-Br	5-*i*Pr	9 ± 0.54	0.21	**20f**	3,4-diCl	5-F	15 ± 1	0.21
11l	4-Br	4,5 Naphthyl[b]	3 ± .14	0.22	**20g**	3,4-diCl	5-Me	7 ± 0.5	0.23
18a	3-Cl	4-Cl	8 ± 0.45	0.23	**20h**	3,4-diCl	6-Me	36 ± 1.5	0.19
18b	3-Cl	5-Cl	ppt[d]	n.c. [e]	**20i**	3,4-diCl	4,5-diMe	62 ± 3.5	0.18
18c	3-Cl	4-Br	6 ± 0.2	0.24	**20j**	3,4-diCl	5-Ethyl	4 ± 0.19	0.23
18d	3-Cl	5-Br	14± 0.5	0.22	**20k**	3,4-diCl	5-*i*Pr	3 ± .012	0.23
18e	3-Cl	4-F	22 ± 3	0.21	**20l**	3,4-diCl	4,5 Naphthyl[b]	1 ± 0.04	0.24
18f	3-Cl	5-F	35 ± 0	0.20					

[a] Average K_d values (n=2) calculated using Cheng-Prusoff equation from IC_{50} values measured in FPA competition assay.

[b] Entire ring system replaces the phenyl.

[c] LE values calculated using LE = 1.4*pK_d/HAC, using the FPA data.

[d] ppt = visible precipitation in assay wells

[e] n.c. = not calculated.

Table 3

SAR of substituents on middle phenyl ring

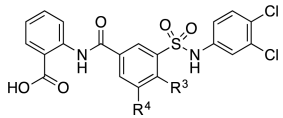

Compd	R_3	R_4	K_d (μM)[a]	LE[b]
20	Me	H	7 ± 3	0.23
20m	H	H	17 ± 1	0.22
20n	Et	H	4 ± 0.25[c]	0.23
20o	*i*Pr	H	5 ± 0.19[c]	0.22
20p	Me	Me	14 ± 1.5	0.21

[a] Average K_d values (n=2) calculated using Cheng-Prusoff equation from IC_{50} values measured in FPA competition assay.

[b] LE values calculated using LE = 1.4*pK_d/HAC, using the FPA data.

[c] Some evidence of precipitation noted at highest concentrations.